

## The Sloan Digital Sky Survey: Technical Summary

Donald G. York<sup>1</sup>, J. Adelman<sup>2</sup>, John E. Anderson, Jr.<sup>2</sup>, Scott F. Anderson<sup>3</sup>, James Annis<sup>2</sup>, Neta A. Bahcall<sup>4</sup>, J. A. Bakken<sup>2</sup>, Robert Barkhouser<sup>5</sup>, Steven Bastian<sup>2</sup>, Eileen Berman<sup>2</sup>, William N. Boroski<sup>2</sup>, Steve Bracker<sup>2</sup>, Charlie Briegel<sup>2</sup>, John W. Briggs<sup>6</sup>, J. Brinkmann<sup>7</sup>, Robert Brunner<sup>8</sup>, Scott Burles<sup>1</sup>, Larry Carey<sup>3</sup>, Michael A. Carr<sup>4</sup>, Francisco J. Castander<sup>1,9</sup>, Bing Chen<sup>5</sup>, Patrick L. Colestock<sup>2</sup>, A. J. Connolly<sup>10</sup>, J. H. Crocker<sup>5</sup>, István Csabai<sup>5,11</sup>, Paul C. Czarapata<sup>2</sup>, John Eric Davis<sup>7</sup>, Mamoru Doi<sup>12</sup>, Tom Dombek<sup>1</sup>, Daniel Eisenstein<sup>13,1,14</sup>, Nancy Ellman<sup>15</sup>, Brian R. Elms<sup>4,16</sup>, Michael L. Evans<sup>3</sup>, Xiaohui Fan<sup>4</sup>, Glenn R. Federwitz<sup>2</sup>, Larry Fiscelli<sup>1</sup>, Scott Friedman<sup>5</sup>, Joshua A. Frieman<sup>2,1</sup>, Masataka Fukugita<sup>17,13</sup>, Bruce Gillespie<sup>7</sup>, James E. Gunn<sup>4</sup>, Vijay K. Gurbani<sup>2</sup>, Ernst de Haas<sup>4</sup>, Merle Haldeman<sup>2</sup>, Frederick H. Harris<sup>18</sup>, J. Hayes<sup>7</sup>, Timothy M. Heckman<sup>5</sup>, G. S. Hennessey<sup>19</sup>, Robert B. Hindsley<sup>20</sup>, Scott Holm<sup>2</sup>, Donald J. Holmgren<sup>2</sup>, Chi-hao Huang<sup>2</sup>, Charles Hull<sup>21</sup>, Don Husby<sup>2</sup>, Shin-Ichi Ichikawa<sup>16</sup>, Takashi Ichikawa<sup>22</sup>, Željko Ivezić<sup>4</sup>, Stephen Kent<sup>2</sup>, Rita S.J. Kim<sup>4</sup>, E. Kinney<sup>7</sup>, Mark Klaene<sup>7</sup>, A. N. Kleinman<sup>7</sup>, S. Kleinman<sup>7</sup>, G. R. Knapp<sup>4</sup>, John Korienek<sup>2</sup>, Richard G. Kron<sup>1,2</sup>, Peter Z. Kunszt<sup>5</sup>, D.Q. Lamb<sup>1</sup>, B. Lee<sup>2</sup>, R. French Leger<sup>3</sup>, Siriluk Limmongkol<sup>3</sup>, Carl Lindenmeyer<sup>2</sup>, Daniel C. Long<sup>7</sup>, Craig Loomis<sup>7</sup>, Jon Loveday<sup>1</sup>, Rich Lucinio<sup>7</sup>, Robert H. Lupton<sup>4</sup>, Bryan MacKinnon<sup>2,23</sup>, Edward J. Mannery<sup>3</sup>, P. M. Mantsch<sup>2</sup>, Bruce Margon<sup>3</sup>, Peregrine McGehee<sup>24</sup>, Timothy A. McKay<sup>25</sup>, Avery Meiksin<sup>26</sup>, Aronne Merelli<sup>27</sup>, David G. Monet<sup>18</sup>, Jeffrey A. Munn<sup>18</sup>, Vijay K. Narayanan<sup>4</sup>, Thomas Nash<sup>2</sup>, Eric Neilsen<sup>5</sup>, Rich Neswold<sup>2</sup>, Heidi Jo Newberg<sup>2,28</sup>, R. C. Nichol<sup>27</sup>, Tom Nicinski<sup>2,29</sup>, Mario Nonino<sup>30</sup>, Norio Okada<sup>16</sup>, Sadanori Okamura<sup>12</sup>, Jeremiah P. Ostriker<sup>4</sup>, Russell Owen<sup>3</sup>, A. George Pauls<sup>4</sup>, John Peoples<sup>2</sup>, R. L. Peterson<sup>2</sup>, Donald Petravick<sup>2</sup>, Jeffrey R. Pier<sup>18</sup>, Adrian Pope<sup>27</sup>, Ruth Pordes<sup>2</sup>, Angela Prosapio<sup>2</sup>, Ron Rechenmacher<sup>2</sup>, Thomas R. Quinn<sup>3</sup>, Gordon T. Richards<sup>1</sup>, Michael W. Richmond<sup>31</sup>, Claudio H. Rivetta<sup>2</sup>, Constance M. Rockosi<sup>1</sup>, Kurt Ruthmansdorfer<sup>2</sup>, Dale Sandford<sup>6</sup>, David J. Schlegel<sup>4</sup>, Donald P. Schneider<sup>32</sup>, Maki Sekiguchi<sup>17</sup>, Gary Sergey<sup>2</sup>, Kazuhiro Shimasaku<sup>12</sup>, Walter A. Siegmund<sup>3</sup>, Stephen Smee<sup>5</sup>, J. Allyn Smith<sup>25</sup>, S. Snedden<sup>7</sup>, R. Stone<sup>18</sup>, Chris Stoughton<sup>2</sup>, Michael A. Strauss<sup>4</sup>, Christopher Stubbs<sup>3</sup>, Mark SubbaRao<sup>1</sup>, Alexander S. Szalay<sup>5</sup>, Istvan Szapudi<sup>33</sup>, Gyula P. Szokoly<sup>5</sup>, Anirudda R. Thakar<sup>5</sup>, Christy Tremonti<sup>5</sup>, Douglas L. Tucker<sup>2</sup>, Alan Uomoto<sup>5</sup>, Dan VandenBerk<sup>2</sup>, Michael S. Vogeley<sup>34</sup>, Patrick Waddell<sup>3</sup>, Shu-i Wang<sup>1</sup>, Masaru Watanabe<sup>35</sup>, David H. Weinberg<sup>36</sup>, Brian Yanny<sup>2</sup>, and Naoki Yasuda<sup>16</sup>  
(The SDSS Collaboration)

- 
- <sup>1</sup>The University of Chicago, Astronomy & Astrophysics Center, 5640 S. Ellis Ave., Chicago, IL 60637
- <sup>2</sup>Fermi National Accelerator Laboratory, P.O. Box 500, Batavia, IL 60510
- <sup>3</sup>University of Washington, Department of Astronomy, Box 351580, Seattle, WA 98195
- <sup>4</sup>Princeton University Observatory, Princeton, NJ 08544
- <sup>5</sup> Department of Physics and Astronomy, The Johns Hopkins University, 3701 San Martin Drive, Baltimore, MD 21218, USA
- <sup>6</sup>Yerkes Observatory, University of Chicago, 373 W. Geneva St. Williams Bay, WI 53191
- <sup>7</sup>Apache Point Observatory, P.O. Box 59, Sunspot, NM 88349-0059
- <sup>8</sup>Department of Astronomy, California Institute of Technology, Pasadena, CA 91125
- <sup>9</sup>Observatoire Midi Pyrenees, 14 ave Edouard Belin, Toulouse, F-31400, France
- <sup>10</sup>Department of Physics and Astronomy, University of Pittsburgh, Pittsburgh, PA 15260
- <sup>11</sup>Department of Physics of Complex Systems, Eötvös University, Pázmány Péter sétány 1/A, Budapest, H-1117, Hungary
- <sup>12</sup>Department of Astronomy and Research Center for the Early Universe, School of Science, University of Tokyo, Hongo, Bunkyo, Tokyo, 113-0033, Japan
- <sup>13</sup>Institute for Advanced Study, Olden Lane, Princeton, NJ 08540
- <sup>14</sup>Hubble Fellow
- <sup>15</sup>Department of Physics, Yale University, PO Box 208121, New Haven, CT 06520-8121
- <sup>16</sup>National Astronomical Observatory, 2-21-1, Osawa, Mitaka, Tokyo 181-8588, Japan
- <sup>17</sup>Institute for Cosmic Ray Research, University of Tokyo, Midori, Tanashi, Tokyo 188-8502, Japan
- <sup>18</sup>U.S. Naval Observatory, Flagstaff Station, P.O. Box 1149, Flagstaff, AZ 86002-1149
- <sup>19</sup>U.S. Naval Observatory, 3450 Massachusetts Ave., NW, Washington, DC 20392-5420
- <sup>20</sup>Remote Sensing Division, Code 7215, Naval Research Laboratory, 4555 Overlook Ave. SW, Washington, DC 20375
- <sup>21</sup>The Observatories of the Carnegie Institution of Washington, 813 Santa Barbara St, Pasadena, CA 91101
- <sup>22</sup>Astronomical Institute, Tohoku University, Aoba, Sendai 980-8578 Japan
- <sup>23</sup>Merrill Lynch, 1-1-3 Otemachi, Chiyoda-ku, Tokyo 100, Japan
- <sup>24</sup>Los Alamos National Laboratory, PO Box 1663, Los Alamos, NM 87545
- <sup>25</sup>University of Michigan, Department of Physics, 500 East University, Ann Arbor, MI 48109
- <sup>26</sup>Royal Observatory, Edinburgh, EH9 3HJ, United Kingdom
- <sup>27</sup>Dept. of Physics, Carnegie Mellon University, 5000 Forbes Ave., Pittsburgh, PA-15232

## ABSTRACT

The Sloan Digital Sky Survey (SDSS) will provide the data to support detailed investigations of the distribution of luminous and non-luminous matter in the Universe: a photometrically and astrometrically calibrated digital imaging survey of  $\pi$  steradians above about Galactic latitude  $30^\circ$  in five broad optical bands to a depth of  $g' \sim 23^m$ , and a spectroscopic survey of the approximately  $10^6$  brightest galaxies and  $10^5$  brightest quasars found in the photometric object catalog produced by the imaging survey. This paper summarizes the observational parameters and data products of the SDSS, and serves as an introduction to extensive technical on-line documentation.

*Subject headings:* instrumentation - - - cosmology: observations

## 1. Introduction

At this writing (May 2000) the Sloan Digital Sky Survey (SDSS) is ending its commissioning phase and beginning operations. The purpose of this paper is to provide a concise summary of the vital statistics of the project, a definition of some of the terms used in the survey and, via links to documentation in electronic form, access to detailed descriptions of the project's design, hardware, and software, to serve as technical background

---

<sup>28</sup>Physics Department, Rensselaer Polytechnic Institute, SC1C25, Troy, NY 12180

<sup>29</sup>Lucent Technologies, 2000 N Naperville Rd, Naperville, IL 60566

<sup>30</sup>Department of Astronomy, Osservatorio Astronomico, via G.B. Tiepolo 11, Trieste 34131, Italy

<sup>31</sup>Physics Department, Rochester Institute of Technology, 85 Lomb Memorial Drive, Rochester, NY 14623-5603

<sup>32</sup>Department of Astronomy and Astrophysics, The Pennsylvania State University, University Park, PA 16802

<sup>33</sup>Canadian Institute for Theoretical Astrophysics, University of Toronto, 60 St. George Street, Toronto, Ontario, M5S 3H8, Canada

<sup>34</sup>Department of Physics, Drexel University, 3141 Chestnut St., Philadelphia, PA 19104

<sup>35</sup> Institute of Space and Astronautical Science Sagamihara, Kanagawa 229, Japan

<sup>36</sup>Ohio State University, Dept. of Astronomy, 140 W. 18th Ave., Columbus, OH 43210

for the project’s science papers. The electronic material is extracted from the text (the “Project Book”) written to support major funding proposals, and is available at the *Astronomical Journal* web site via the on-line version of this paper. The official SDSS web site (<http://www.sdss.org>) also provides links to the on-line Project Book, and it can be accessed directly at <http://www.astro.princeton.edu/PBOOK/welcome.htm>. In the discussion below we reference the chapters in the Project Book by the last part of the URL, i.e. that following PBOOK/. The versions accessible at the SDSS web sites also contain extensive discussions and summaries of the scientific goals of the survey, which are not included here.

The text of the on-line Project Book was last updated in August 1997. While there have been a number of changes in the hardware and software described therein, the material accurately describes the design goals and the implementation of the major observing subsystems. As the project becomes operational, we will provide a series of formal technical papers (most still in preparation), which will describe in detail the project hardware and software in its actual operational state.

Section 2 describes the Survey’s objectives: the imaging depth, sky coverage, and instrumentation. Section 3 summarizes the software and data reduction components of the SDSS and its data products. Section 4 reviews some recent scientific results from the project’s initial commissioning data runs, which demonstrate the ability of the project to reach its technical goals. All Celestial coordinates are in epoch J2000.

## 2. Survey Characteristics

The Sloan Digital Sky Survey will produce both imaging and spectroscopic surveys over a large area of the sky. The survey uses a dedicated 2.5 m telescope equipped with a large format mosaic CCD camera to image the sky in five optical bands, and two digital spectrographs to obtain the spectra of about one million galaxies and 100,000 quasars selected from the imaging data.

The SDSS calibrates its photometry using observations of a network of standard stars established by the United States Naval Observatory (USNO) 1 m telescope, and its astrometry using observations by an array of astrometric CCDs in the imaging camera.

### 2.1. Telescope

The SDSS telescope is a 2.5m f/5 modified Ritchey-Chrétien wide-field altitude-azimuth telescope (see <telescop/telescop.htm>) located at the Apache Point Observatory (APO),

Sunspot, New Mexico ([site/site.htm](#)). The telescope achieves a very wide ( $3^\circ$ ) distortion-free field by the use of a large secondary mirror and two corrector lenses. It is equipped with the photometric/astrometric mosaic camera ([camera/camera.htm](#), Gunn et al. 1998) and images the sky by scanning along great circles at the sidereal rate. The imaging camera mounts at the Cassegrain focus. The telescope is also equipped with two double fiber-fed spectrographs, permanently mounted on the image rotator, since the spectrographs are fiber fed. This ensures that the fibers do not flex during an exposure. The telescope is changed from imaging mode to spectroscopic mode by removing the imaging camera and mounting at the Cassegrain focus a fiber plug plate, individually drilled for each field, which feeds the spectrographs. In survey operations, it is expected that up to nine spectroscopic plates per night will be observed, with the necessary plates being plugged with fibers during the day. The telescope mounting and enclosure allow easy access for rapid changes between fiber plug plates and between spectroscopic and imaging modes. This strategy allows imaging to be done in pristine observing conditions (photometric sky, image size  $\leq 1.5''$  FWHM) and spectroscopy to be done during less ideal conditions. All observing will be done in moonless sky.

Besides the 2.5m telescope, the SDSS makes use of three subsidiary instruments at the site. The *Photometric Telescope* (PT) is a 0.5m telescope equipped with a CCD camera and the SDSS filter set. Its task is to calibrate the photometry. Two instruments, a *seeing monitor* and a  $10\mu\text{m}$  *cloud scanner* (Hull et al. 1995; [site/site.htm](#)) monitor the astronomical weather.

## 2.2. Imaging Camera

The SDSS imaging camera contains two sets of CCD arrays: the imaging array and the astrometric arrays ([camera/camera.htm](#), Gunn et al. 1998).

The *imaging array* consists of 30  $2048 \times 2048$  Tektronix CCDs, placed in an array of six columns and five rows. The telescope scanning is aligned with the columns. Each row observes the sky through a different filter, in temporal sequence  $r', i', u', z'$ , and  $g'$ . The pixel size is  $24\mu\text{m}$  ( $0.396''$  on the sky). The imaging survey is taken in drift-scan (time-delay-and-integrate, or TDI) mode, i.e. the camera continually sweeps the sky in great circles, and a given point on the sky passes through the five filters in succession. The effective integration time per filter is 54.1 seconds, and the time for passage over the entire photometric array is about 5.7 minutes ([strategy/strategy.htm](#); Gunn et al. 1998). Since the camera contains six columns of CCDs, the result is a long *strip* of six *scanlines*, containing almost simultaneously observed five-color data for each of the six CCD columns. Each CCD

observes a swath of sky  $13.52'$  wide. The CCDs are separated in the *row* direction (i.e. perpendicular to the scan direction) by  $91.0$  mm ( $25.2'$  on the sky) center-to-center. The observations are filled in by a second strip, offset from the first by 93% of the CCD width, to produce a filled *stripe*,  $2.54^\circ$  wide, with 8% ( $1'$ ) lateral overlap on each side. Because of the camera's large field of view, the TDI tracking must be done along great circles. The Northern Galactic Cap is covered by 45 great-circle arcs (shown projected on the sky in Figures 1 and 2).

### 2.3. Photometry and Photometric Calibration

The five filters in the imaging array of the camera, [ $u'$ ,  $g'$ ,  $r'$ ,  $i'$  and  $z'$ ] have effective wavelengths of [ $3590 \text{ \AA}$ ,  $4810 \text{ \AA}$ ,  $6230 \text{ \AA}$ ,  $7640 \text{ \AA}$  and  $9060 \text{ \AA}$ ] (Fukugita et al. 1996; Gunn et al. 1998). An a priori model estimate of the telescope and camera throughputs and of the sky brightness predicted that we would reach the  $5\sigma$  detection limit for point sources in  $1''$  seeing at [22.3, 23.3, 23.1, 22.3, 20.8] in the ( $u'$ ,  $g'$ ,  $r'$ ,  $i'$ ,  $z'$ ) filters, respectively, at an airmass of 1.4. We have put formal requirements on throughput at 75% of the values used for the above estimation, and have demonstrated that we meet this requirement in all bands with the possible exception of  $z'$ . The sensitivity limit can be tested by finding the magnitude at which repeat observations of a given area of sky yield 50% reproducibility of the objects detected. This has been tested most thoroughly with data taken in less than optimal seeing ( $1.3'' - 1.6''$ ); nevertheless, the 50% reproducibility level lies within a few tenths of a magnitude of the above-quoted  $5\sigma$  detection limit in all five bands (see Ivezić et al. 2000). The SDSS science requirements demand that photometric calibration uncertainties for point sources be 0.02 in  $r'$ , 0.02 in  $r' - i'$  and  $g' - r'$ , and 0.03 in  $u' - g'$  and  $i' - z'$ . To meet these stringent requirements in both signal-to-noise ratio and photometricity, imaging data are declared to be survey quality only if the PT determines that the night is photometric, with a zero-point uncertainty below 1%, and if the seeing is better than  $1.5''$ . The imaging data saturate at about [13, 14, 14, 14, 12] magnitudes for point sources.

The magnitude scale is on the  $AB_\nu$  system (Oke 1969, unpublished), which was updated to the  $AB_{79}$  system by Oke & Gunn (1983) and to  $AB_{95}$  by Fukugita et al. (1996). The magnitudes  $m$  are related to flux density  $f$  by  $m \sim \sinh^{-1}(f)$  rather than logarithmically (see Lupton, Gunn & Szalay 1999 and Fan et al. 1999). This definition is essentially identical to the logarithmic magnitude at signal-to-noise ratios greater than about 5 and is well behaved for low and even zero and negative flux densities.

The calibration and definition of the magnitude system is carried out by the USNO 1 m telescope and the 0.5m PT. The SDSS photometry is placed on the  $AB_\nu$  system using three

*fundamental standards* (BD + 17°4708, BD + 26°2606, and BD + 21°609), whose magnitude scale is as defined by Fukugita et al. (1996); a set of 157 *primary standards*, which are calibrated by the above fundamental standards using the USNO 1m telescope, and which cover the whole range of right ascension and enable the calibration system to be made self-consistent; and a set of *secondary calibration patches* lying across the imaging stripes, containing stars fainter than 14<sup>m</sup> whose magnitudes are calibrated by the PT with respect to those of the primary standards and which transfer that calibration to the imaging survey. The locations of these patches on the survey stripes are shown in Figure 1. On nights when the 2.5 m is observing, the PT observes primary standard stars to provide the atmospheric extinction coefficients over the night and to confirm that the night is photometric. The standard star network is described in [photcal/photcal.htm](#) — note that the telescope described there has now been replaced by the 0.5m PT.

#### 2.4. Astrometric Calibration

The camera also contains leading and trailing *astrometric arrays* — narrow (128×2048), neutral-density-filtered, *r'*-filtered CCDs covering the entire width of the camera. These arrays can measure objects in the magnitude range  $r' \sim 8.5 - 16.8$ , i.e. they cover the dynamic range between the standard astrometric catalog stars and the brightest unsaturated stars in the photometric array. The astrometric calibration is thereby referenced to the fundamental astrometric catalogues (see [astrom/astrom.htm](#)), using the Hipparcos and Tycho Catalogues (ESA 1997) and specially observed equatorial fields (Stone et al. 1999). Comparison with positions from the FIRST (Becker et al. 1995) and 2MASS (Skrutskie 1999) catalogues shows that the rms astrometric accuracy is currently better than 150 milliarcseconds (mas) in each coordinate.

#### 2.5. Imaging Survey: North Galactic Cap

The imaging survey covers about 10,000 contiguous square degrees in the Northern Galactic Cap. This area lies basically above Galactic latitude 30°, but its footprint is adjusted slightly to lie within the minimum of the Galactic extinction contours (Schlegel, Finkbeiner & Davis 1998), resulting in an elliptical region. The region is centered at  $\alpha = 12^h 20^m$ ,  $\delta = +32.5^\circ$ . The minor axis is at an angle 20° East of North with extent  $\pm 55^\circ$ . The major axis is a great circle perpendicular to the minor axis with extent  $\pm 65^\circ$ . The survey footprint with the location of the stripes is shown in Figure 2 — see [strategy/strategy.htm](#) for details.

## 2.6. Imaging Survey: The South Galactic Cap

In the South Galactic Cap, three stripes will be observed, one along the Celestial Equator and the other two north and south of the equator (see Figure 2). The *equatorial stripe* ( $\alpha = 20.7^h$  to  $4^h$ ,  $\delta = 0^\circ$ ) will be observed repeatedly, both to find variable objects and, when co-added, to reach magnitude limits about  $2^m$  deeper than the Northern imaging survey.

The other two stripes will cover great circles lying between  $\alpha$ ,  $\delta$  of  $(20.7^h, -5.8^\circ \rightarrow 4.0^h, -5.8^\circ)$  and  $(22.4^h, 8.7^\circ \rightarrow 2.3^h, 13.2^\circ)$ .

## 2.7. The Spectroscopic Survey

Objects are detected in the imaging survey, classified as point source or extended, and measured, by the image analysis software (see below). These imaging data are used to select in a uniform way different classes of objects whose spectra will be taken. The final details of this *target selection* will be described once the survey is well underway; the criteria discussed here are likely to be very close to those finally used.

Two samples of *galaxies* are selected from the objects classified as “extended”. About  $9 \times 10^5$  galaxies will be selected to have Petrosian (1976) magnitudes  $r'_P \leq 17.7$ . Galaxies with a mean  $r'$  band surface brightness within the half light radius fainter than 24 magnitudes/arc second<sup>2</sup> will be removed, since spectroscopic observations are unlikely to produce a redshift. For illustrative purposes, a simulation of a slice of the SDSS redshift survey is shown in Figure 3 (from Colley et al. 2000). Galaxies in this CDM simulation are ‘selected’ by the SDSS selection criteria. As Figure 3 demonstrates, the SDSS volume is large enough to contain a statistically significant sample of the largest structures predicted.

The second sample, of approximately  $10^5$  galaxies, exploits the characteristic very red color and high metallicity (producing strong absorption lines) of the most luminous galaxies: the “Brightest Cluster Galaxies” or “Bright Red Galaxies” (BRGs); redshifts can be well measured with the SDSS spectra for these galaxies to about  $r' = 19.5$ . Galaxies located at the dynamical centers of nearby dense clusters often have these properties. Reasonably accurate photometric redshifts (Connolly et al. 1995) can be determined for these galaxies, allowing the selection by magnitude and  $g'r'i'$  color of an essentially *distance limited* sample of the highest-density regions of the Universe to a redshift of about 0.45 (see Figure 4 for a simulation).

With their power-law continua and the influence of Lyman- $\alpha$  emission and the Lyman- $\alpha$  forest, *quasars* have  $u'g'r'i'z'$  colors quite distinct from those of the vastly more numerous

stars over most of their redshift range (Fan 1999). Thus about  $1.5 \times 10^5$  *quasar candidates* are selected for spectroscopic observations as outliers from the stellar locus (cf., Krisciunas et al. 1998; Lenz et al. 1998; Newberg et al. 1999; Figure 5 below) in color-color space. At the cost of some loss of efficiency, selection is allowed closer to the stellar locus around  $z = 2.8$ , where quasar colors approach those of early F and late A stars (Newberg & Yanny 1997; Fan 1999). Some further regions of color-color space outside the main part of the stellar locus where quasars are very rarely found are also excluded, including the regions containing M dwarf-white dwarf pairs, early A stars, and white dwarfs (see Figure 5). The SDSS will compile a sample of quasars brighter than  $i' \approx 19$  at  $z < 3.0$ ; at redshifts between 3.0 and about 5.2, the limiting magnitude will be about  $i' = 20$ . Objects are also required to be point sources, except in the region of color-color space where low-redshift quasars are expected to be found. Stellar objects brighter than  $i' = 20$  which are FIRST sources (Becker, White and Helfand 1995) are also selected. Based on early spectroscopy, we estimate that roughly 65% of our quasar candidates are genuine quasars; comparison with samples of known quasars indicates that our completeness is of order 90%.

In all cases, the magnitudes of the objects are corrected for Galactic extinction before selection, using extinction in the SDSS bands calculated from the reddening map of Schlegel, Finkbeiner & Davis (1998). Objects are then selected to have a magnitude limit *outside* the Galaxy. If this correction were not made, the systematic effects of Galactic extinction over the survey area would overwhelm the statistical uncertainties in the SDSS data set. After the imaging and spectroscopic survey is completed in a given part of the sky, the reddening and extinction will be recalculated using internal standards extracted from the imaging data. The SDSS plans to use a variety of extinction probes, including very hot halo subdwarfs, halo turnoff stars, and elliptical galaxies whose intrinsic colors can be estimated from their line indices.

Together with various classes of calibration stars and fibers which observe blank sky to measure the sky spectrum, the selected galaxies and quasars are mapped onto the sky, and ‘tiled’, i.e. their location on a  $3^\circ$  diameter plug plate determined (`tiling/tiling.htm`). The centers of the tiles are adjusted to provide closer coverage of regions of high galactic surface density, to make the spectroscopic coverage optimally uniform. Excess fibers are allocated to several classes of rare or peculiar objects (for example objects which are positionally matched with ROSAT sources, or those whose parameters lie outside any known range – these are *serendipitous* objects) and to samples of stars. The spectra are observed, 640 at a time (with a total integration time of 45 - 60 minutes depending on observing conditions) using a pair of fiber-fed double spectrographs (`spectro/spectro.htm`). The wavelength coverage of the spectrographs is continuous from about 3800 Å to 9200 Å, and the wavelength resolution,  $\lambda/\delta\lambda$ , is 1800 (Uomoto et al. 1999). The fibers are located at the focal plane via plug

plates constructed for each area of sky. The fiber diameter is 0.2 mm ( $3''$  on the sky), and adjacent fibers cannot be located more closely than  $55''$  on the sky. Both members of a pair of objects closer than this separation can be observed spectroscopically if they are located in the overlapping regions of adjacent tiles.

Tests of the redshift accuracy using observations of stars in M67 whose radial velocities are accurately known (Mathieu et al. 1986) show that the SDSS radial velocity measurements for stars have a scatter of about  $3.5 \text{ km s}^{-1}$ .

### 3. Software and Data Products

The operational software is described in `datasys/datasys.htm`. The data are obtained using the Data Acquisition (DA) system at APO (Petraevick et al. 1994) and recorded on DLT tape. The imaging data consist of full images from all CCDs of the imaging array, cut-outs of detected objects from the astrometric array, and bookkeeping information. These tapes are shipped to Fermilab by express courier and the data are automatically reduced through an interoperating set of software pipelines operating in a common computing environment.

The *photometric pipeline* reduces the imaging data; it corrects the data for data defects (interpolation over bad columns and bleed trails, finding and interpolating over ‘cosmic rays’, etc), calculates overscan (bias), sky and flat field values, calculates the point spread functions (psf) as a function of time and location on the CCD array, finds objects, combines the data from the five bands, carries out simple model fits to the images of each object, deblends overlapping objects, and measures positions, magnitudes (including psf and Petrosian magnitudes) and shape parameters. The photometric pipeline uses position calibration information from the astrometric array reduced through the *astrometric pipeline* and photometric calibration data from the photometric telescope (reduced through the *photometric telescope pipeline*). Final calibrations are applied by the *final calibration pipeline*, which allows refinements in the positional and photometric calibration as the survey progresses. The photometric pipeline is extensively tested using repeat observations, examination of the outputs, observations of regions of the sky previously observed by other telescopes (HST fields, for example) and a set of simulations, described in detail in `simul/simul.htm`. For an example of the repeatability of SDSS photometry over several timescales, see Ivezić et al. (2000). These repeat observations show that the mean errors (for point sources) are about  $0.03^m$  to  $20^m$ , increasing to about  $0.05^m$  at  $21^m$  and to  $0.12^m$  at  $22^m$ . These observed errors are in good agreement with those quoted by the photometric pipeline. They apply only to the  $g'$ ,  $r'$  and  $i'$  bands – in the less sensitive  $u'$  and  $z'$  bands, the errors at the bright end are about the same as those in  $g'r'i'$ , but increase to  $0.05^m$  at  $20^m$  and  $0.12^m$  at  $21^m$ .

The outputs, together with all the observing and processing information, are loaded into the *operational data base* which is the central collection of scientific and bookkeeping data used to run the survey. To select the spectroscopic targets, objects are run through the *target selection pipeline* and flagged if they meet the spectroscopic selection criteria for a particular type of object. The criteria for the primary objects (quasars, galaxies and BRGs) will not be changed once the survey is underway. Those for serendipitous objects and samples of interesting stars can be changed throughout the survey. A given object can in principle receive several target flags. The selected objects are tiled as described above, plug plates are drilled, and the spectroscopic observations are made. The spectroscopic data are automatically reduced by the *spectroscopic pipeline*, which extracts, corrects and calibrates the spectra, determines the spectral types, and measures the redshifts. The reduced spectra are then stored in the operational data base. The contents of the operational data base are copied at regular intervals into the *science data base* for retrieval and scientific analysis (see [appsoft/appsoft.htm](http://appsoft/appsoft.htm)). The science data base is indexed in a hierarchical manner: the data and other information are linked into ‘containers’ that can be divided and subdivided as necessary, to define easily searchable regions with approximately the same data content. This hierarchical scheme is consistent with those being adopted by other large surveys, to allow cross referencing of multiple surveys. The science data base also incorporates a set of query tools and is designed for easy portability.

The photometric data products of the SDSS include: a *catalog* of all detected objects, with measured positions, magnitudes, shape parameters, model fits and processing flags; *atlas images* (i.e. cutouts from the imaging data in all five bands) of all detected objects and of objects from the FIRST and ROSAT catalogs; a  $4 \times 4$  binned image of the corrected images with the objects removed; and a *mask* of the areas of sky not processed (because of saturated stars, for example) and of corrected pixels (e.g. those from which cosmic rays were removed). The atlas images are sized to enclose the area occupied by each object plus the PSF width, or the object size given in the ROSAT or FIRST catalogues. The photometric outputs are described in <http://www.astro.princeton.edu/SDSS/photo.html>. The data base will also contain the calibrated 1D *spectra*, the derived *redshift* and *spectral type*, and the bookkeeping information related to the spectroscopic observations. In addition, the positions of astrometric calibration stars measured by the astrometric pipeline and the magnitudes of the faint photometric standards measured by the photometric telescope pipeline will be published at regular intervals.

#### 4. Early Science from the SDSS Commissioning Data

The goal of the SDSS is to provide the data necessary for studies of the large scale structure of the Universe on a wide range of scales. The imaging survey should detect  $\sim 5 \times 10^7$  galaxies,  $\sim 10^6$  quasars and  $\sim 8 \times 10^7$  stars to the survey limits. These photometric data, via photometric redshifts and various statistical techniques such as the angular correlation function, support studies of large scale structure well past the limit of the spectroscopic survey. On even larger scales, information on structure will come from quasars.

The science justification for the SDSS is discussed in several conference papers (e.g. Gunn & Weinberg 1995; Fukugita 1998; Margon 1999). The Project Book science sections can be accessed at <http://www.astro.princeton.edu/PBOOK/science/science.htm>. Much of the science for which the SDSS was built, the study of large scale structure, will come when the survey is complete, but the initial test data have already led to significant scientific discoveries in many fields. In this section, we show examples of the first test data and some initial results. To date (May 2000), the SDSS has obtained test imaging data for some 2000 square degrees of sky and about 20,000 spectra. Examples of these data are shown in Figures 5 (sample color-color and color-magnitude diagrams of point-source objects), 6 (sample spectra) and 7 (a composite color image of a piece of the sky which contains the cluster Abell 267),

Fischer et al. (2000) have detected the signature of the weak lensing of background galaxies by foreground galaxies, allowing the halos and total masses of the foreground galaxies to be measured.

The searches by Fan et al. (1999a,b; 2000a,c), Schneider et al. (2000) and Zheng et al. (2000) have greatly increased the number of known high redshift ( $z > 3.6$ ) quasars and include several quasars with  $z > 5$ . Fan et al. (1999b) have found the first example of a new kind of quasar: a high redshift object with a featureless spectrum and without the radio emission and polarization characteristics of BL Lac objects. The redshift for this object ( $z = 4.6$ ) is found from the Lyman- $\alpha$  forest absorption in the spectrum.

Some 150 distant probable RR Lyrae stars have been found in the Galactic halo, enabling the halo stellar density to be mapped; the distribution may have located the edge of the halo at approximately 60 kpc (Ivezić et al. 2000). The distribution of RR Lyrae stars and other horizontal branch stars is very clumped, showing the presence of possible tidal streamers in the halo (Ivezić et al. 2000; Yanny et al. 2000). Margon et al. (1999) describe the discovery of faint high latitude carbon stars in the SDSS data.

Strauss et al. (1999), Schneider et al. (2000), Fan et al. (2000b), Tsvetanov et al. (2000), Pier et al. (2000) and Leggett et al. (2000) report the discovery of a number of

very low mass stars or substellar objects, those of type ‘L’ or ‘T’, including the first field methane (‘T’) dwarfs and the first stars of spectral type intermediate between ‘L’ and ‘T’. The detection rate to date shows that the SDSS is likely to identify several thousand L and T dwarfs. These objects are found to occupy very distinct regions of color-color and color-magnitude space, which will enable the completeness of the samples to be well characterized.

Measurements of the psf diameter variations and the image wander allow variations in the turbulence in the Earth’s atmosphere to be tracked. These data demonstrate the presence of anomalous refraction on scales at least as large as the  $2.3^\circ$  field of view of the camera (Pier et al. 1999).

Of course the most exciting possibility for any large survey which probes new regions of sensitivity or wavelength is the discovery of exceedingly rare or entirely new classes of objects. The SDSS has already found a number of very unusual objects; the nature of some of these remains unknown (Fan et al. 1999c). These and other investigations in progress show the promise of SDSS for greatly advancing astronomical work in fields ranging from the behavior of the Earth’s atmosphere to structure on the scale of the horizon of the Universe.

The Sloan Digital Sky Survey (SDSS) is a joint project of The University of Chicago, Fermilab, the Institute for Advanced Study, the Japan Participation Group, The Johns Hopkins University, the Max-Planck-Institute for Astronomy, Princeton University, the United States Naval Observatory, and the University of Washington. Apache Point Observatory, site of the SDSS, is operated by the Astrophysical Research Consortium. Funding for the project has been provided by the Alfred P. Sloan Foundation, the SDSS member institutions, the National Aeronautics and Space Administration, the National Science Foundation, the U.S. Department of Energy, and Monbusho. The official SDSS web site is [www.sdss.org](http://www.sdss.org).

## REFERENCES

- Bade, N., Engels, D., Voges, W., et al. 1998, *A&AS*, 127, 145  
Becker, R.H., White, R.L., & Helfand, D.J. 1995, *ApJ*, 450, 559  
Berger, J., & Fringant, A.-M., 1985, *A&AS*, 61, 191  
Colley, W. N., Gott, J. R., Weinberg, D. H., Park, C., & Berlind, A. A. 2000, *ApJ*, 529, 795  
Connolly, A.J., Csabai, I., Szalay, A.S., Koo, D.C., Kron, R.G., & Munn, J.A. 1995, *AJ*, 110, 2655  
Crawford, C.S., Allen, S.W., Ebeling, H., A.C., & Fabian, A.C. 1999, *MNRAS*, 306, 857

- ESA 1997, The Hipparcos and Tycho Catalogues, ESA SP-1020
- Fan, X. 1999, AJ, 117, 2528
- Fan, X., Strauss, M. A., Schneider, D.P., et al. 1999a, AJ, 118, 1
- Fan, X., Strauss, M.A., Gunn, J.E. et al. 1999b, ApJ 526, L57
- Fan, X., Strauss, M.A., Schneider, D.P., Gunn, J.E., Lupton, R.L., Knapp, G.R., & Yanny, B. 1999c, AAS, 73.15
- Fan, X., Strauss, M. A., Schneider, D.P., et al. 2000a, AJ, 119, 1
- Fan, X., Knapp, G.R., Strauss, M.A., et al. 2000b, AJ, 119, 928
- Fan, X., White, R.L., Davis, M., et al. 2000c, submitted to AJ
- Fischer, P., McKay, T., Sheldon, E. et al. 2000, submitted to AJ (astro-ph/9912119)
- Fukugita, M. 1998, in Highlights of Astronomy, 11A, ed. J Andersen, 449.
- Fukugita, M., Ichikawa, T., Gunn, J.E., Doi, M., Shimasaku, K., & Schneider, D.P. 1996, AJ, 111, 1748
- Gunn, J.E., Carr, M.A., Rockosi, C.M., Sekiguchi, M., et al. 1998, AJ, 116, 3040
- Gunn, J.E., & Weinberg, D.H. 1995, in “Wide Field Spectroscopy and the Distant Universe”, ed. S. Maddox & A. Aragòn-Salamanca, World Scientific (Singapore), 3
- Hull, C., Limmongkol, S., & Siegmund, W. 1994, Proc. S.P.I.E., 2199
- Ivezić, Ž., Goldston, J., Finlator, K., et al. 2000, AJ (in press: astro-ph/0004130)
- Krisciunas, K., Margon, B., & Szkody, P. 1998, PASP, 110, 1342
- Lenz, D.D., Newberg, H.J., Rosner, R., Richards, G.T., & Stoughton, C. 1998, ApJS, 119, 121
- Lupton, R.H., Gunn, J.E., & Szalay, A. 1999, AJ, 118, 1406
- Mathieu, R.D., Latham, D.W., Griffin, R.F., & Gunn, J.E. 1986, AJ, 92, 1100
- Margon, B. 1999, Philosophical Transactions of the Royal Society of London A, 357, 93.
- Margon, B., Anderson, S.F., Deutsch, E., & Harris, H. 1999, BAAS 195.8006
- Morris, S.L., Weymann, R.J., Anderson, S.F., Hewett, P.C., Foltz, C.B., Chaffee, F.H., Francis, P.J., & MacAlpine, G.M. 1991, AJ, 102, 1627
- Newberg, H.J., & Yanny, B. 1997, ApJS, 113, 89
- Newberg, H.H., Richards, G.T., Richmond, M.W., & Fan, X. 1999, ApJS, 123, 377
- Oke, J.B., & Gunn, J.E. 1983, ApJ, 266, 713

- Petravick, D., et al. 1994, S.P.I.E., 2198, 935
- Petrosian, V. 1976, ApJ, 209, L1
- Pier, J.R., Leggett, S.K., Strauss, M.A., et al. 2000, in “From Giant Planets to Cool Stars”, ed.C. Griffith & M. Marley, ASP Conf. Ser., in press
- Pier, J.R., Munn, J.A., Hennessy, G.S., Hindsley, R.H., & Kent, S.M. 1999, AAS, 195, 81.04
- Schlegel, D.J., Finkbeiner, D.P., & Davis, M. 1998, ApJ, 500, 525
- Schneider, D.P., Hill, G.J., Fan, X., et al. 2000, PASP, 112, 6
- Skrutskie, M.F. 1999, AAS, 195, 34.01
- Strauss, M.A., Fan, X., Gunn, J.E., et al., 1999, ApJ, 522, L61
- Stone, R.C., Pier, J.R., & Monet, D.G. 1999, AJ, 118, 2488
- Tsvetanov, Z.I., Golimowski, D., Zheng, W., et al. 2000, ApJ, 513, L61
- Uomoto, A., Smee, S., Rockosi, C., Burles, S., Pope, A., Friedman, S., Brinkmann, J., Gunn, J.E., & Nichol, R, 1999, AAS, 195.87.01
- Yanny, B., Newberg, H., Kent, S., et al. 2000, AJ (in press: astro-ph/0004128)
- Zheng, W., Tsvetanov, Z.I., Schneider, D.P., et al. 2000, submitted to AJ (astro-ph/0005247)

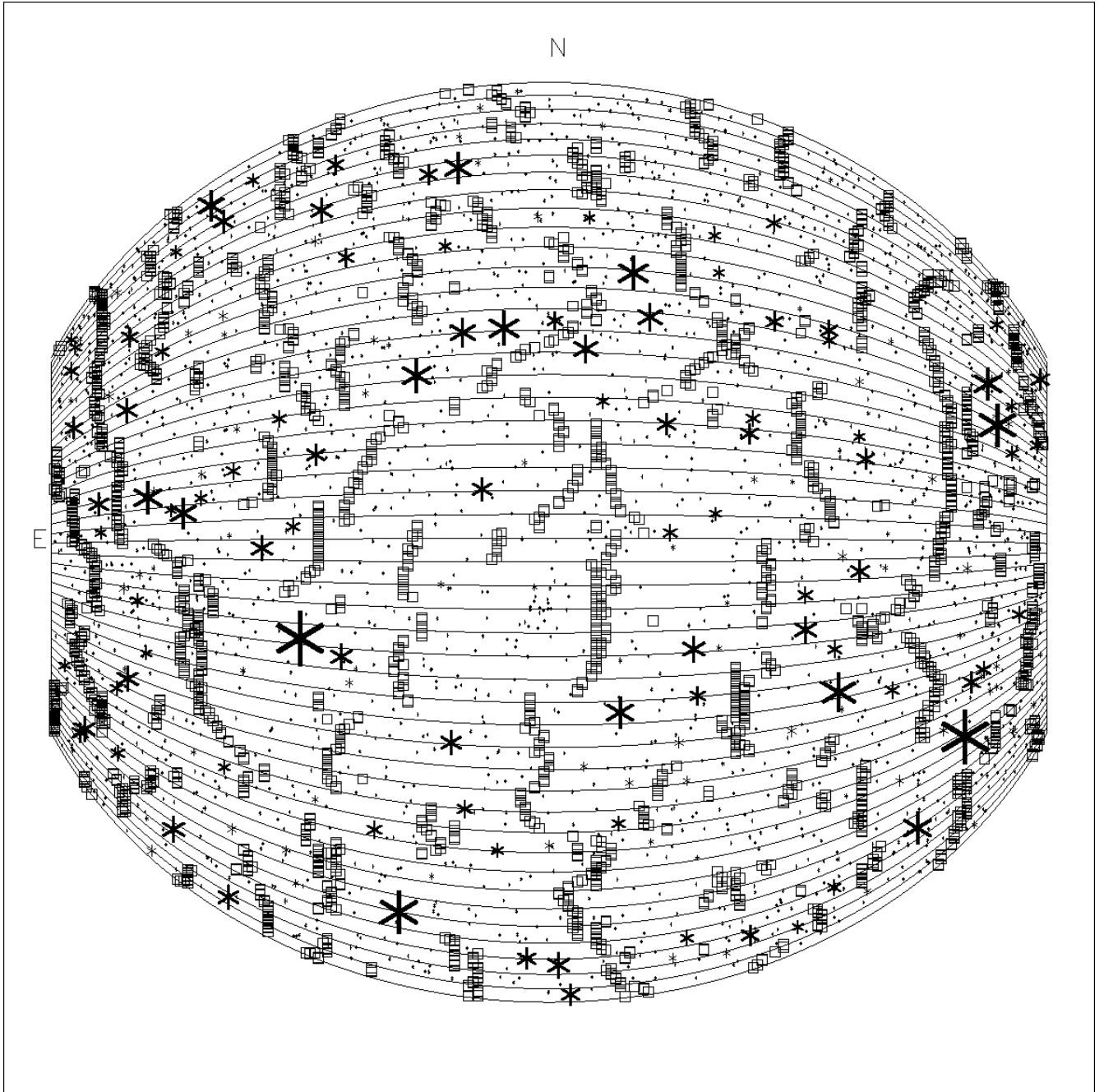


Figure 1. Projection on the sky of the northern SDSS survey area. The positions of the Yale Bright Star Catalogue stars are shown. The largest symbols are stars of  $0^m$  and the smallest stars of  $5^m - 7^m$ . The secondary calibration patches are shown by squares.

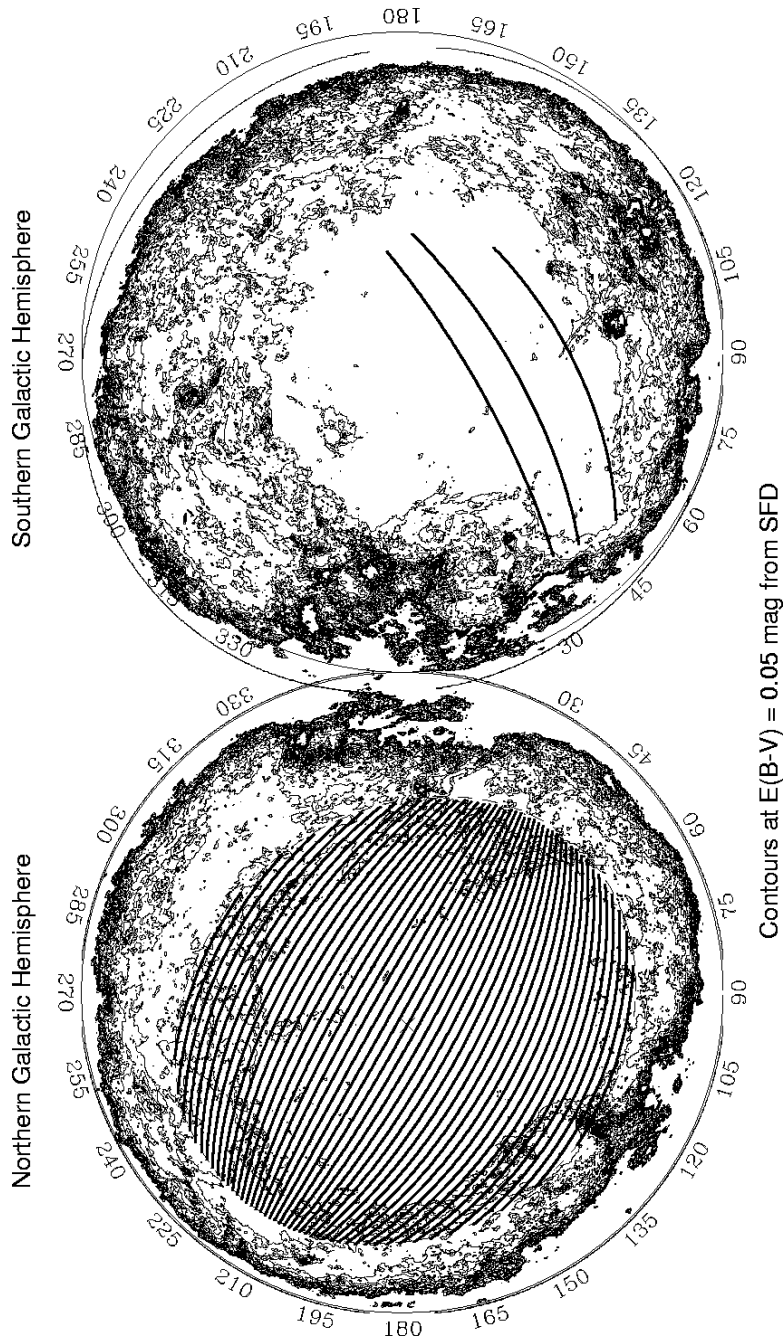
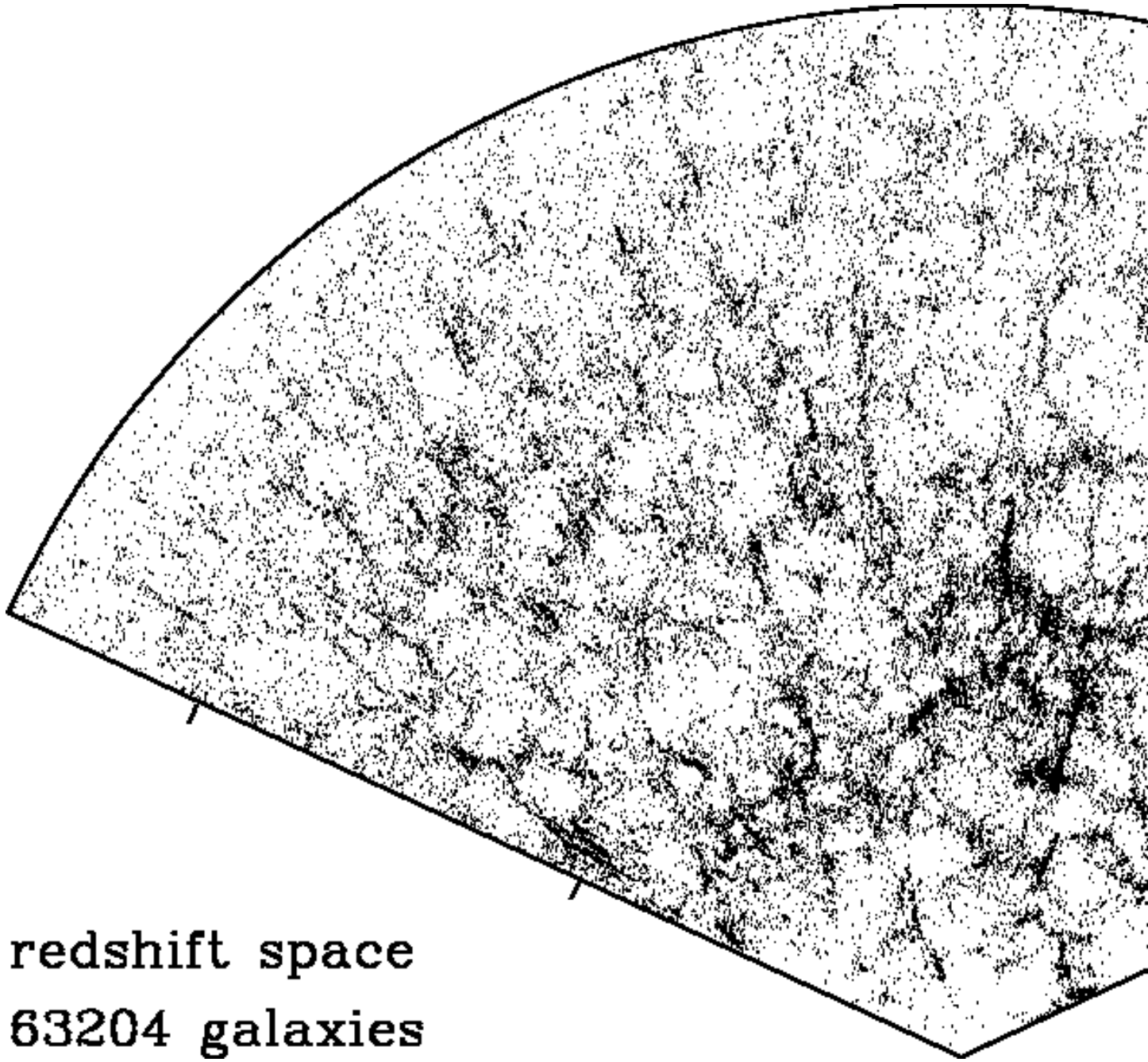


Figure 2. Projection on the sky (Galactic coordinates) of the Northern and Southern SDSS surveys. The lines show the individual stripes to be scanned by the imaging camera. These are overlaid on the extinction contours of Schlegel, Finkbeiner and Davis (1998). The Survey pole is marked by the 'X'.



**redshift space**  
**63204 galaxies**

Figure 3. A six-degree wide slice of the Simulated Sloan Digital Sky Survey (from Colley et al. 2000), showing about 1/20 of the survey.

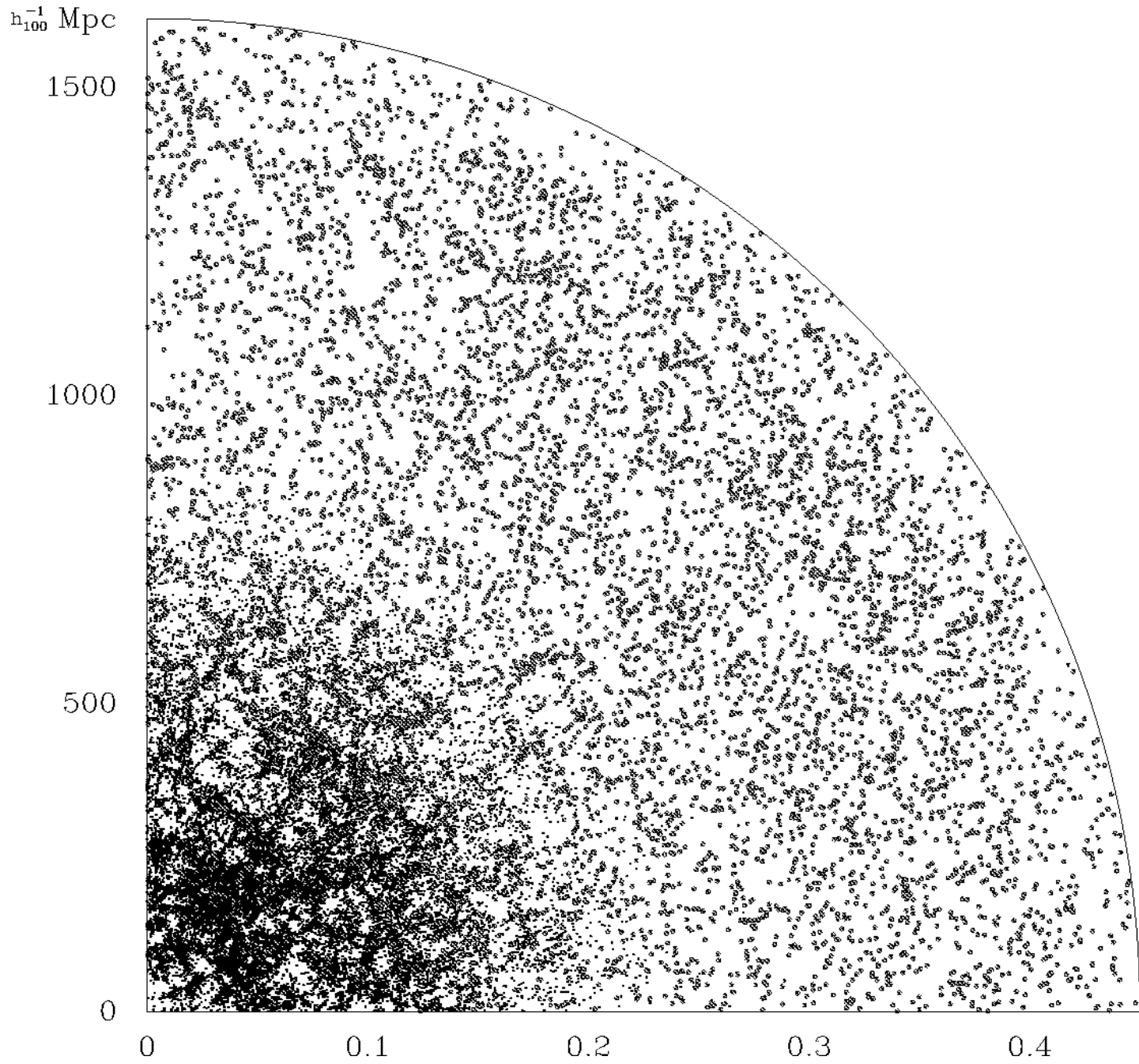


Figure 4. Simulated redshift distribution in a  $6^\circ$  slice of the SDSS. Small dots: main galaxy sample (cf. Figure 3). Large dots: the BRG sample, showing about 1/30 of the survey.

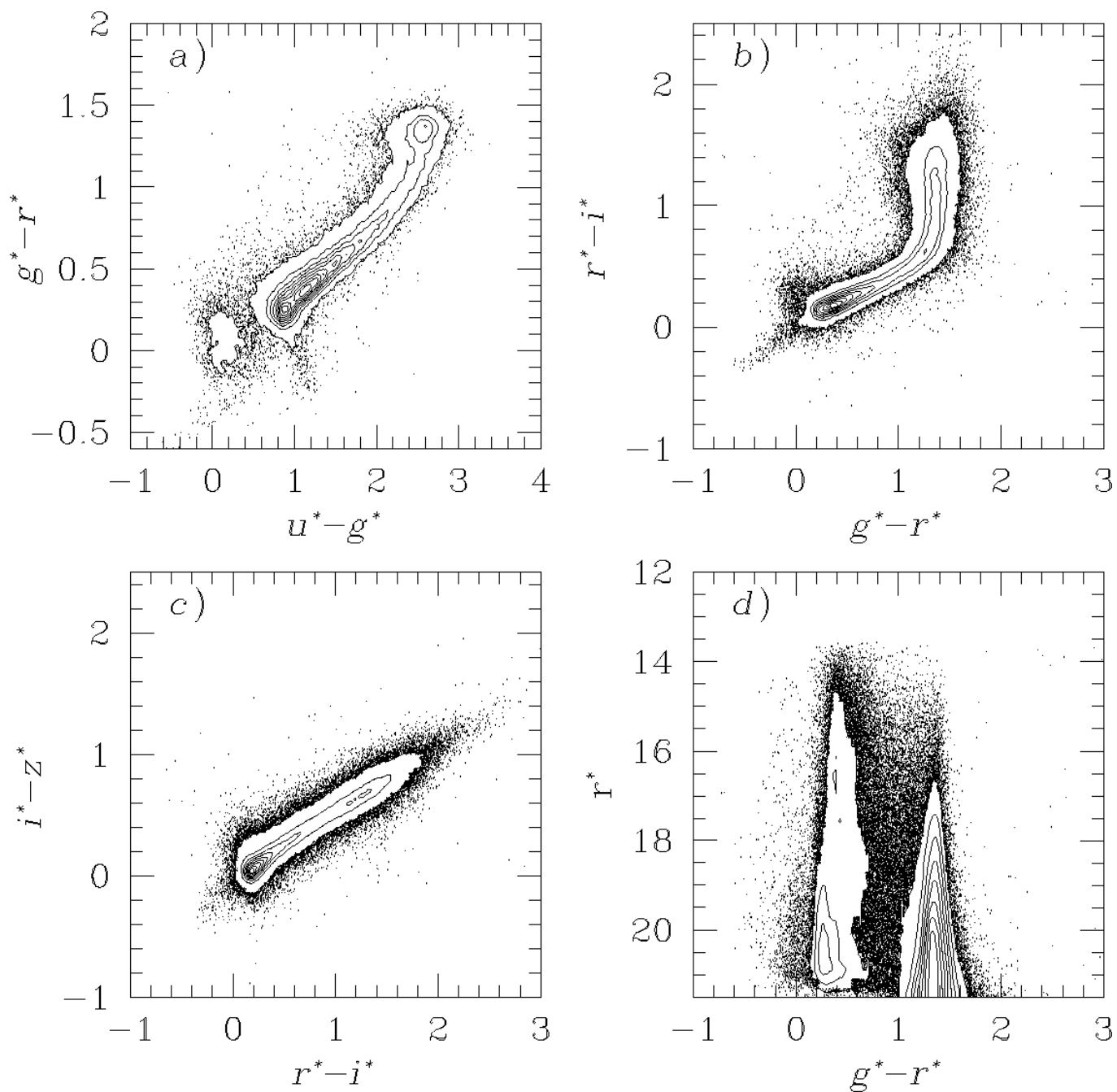


Figure 5. Color-color and color-magnitude plots of about 117,000 point sources brighter than  $21^m$  at  $i^*$  and detected at greater than  $5\sigma$  in each band from 25 square degrees of SDSS imaging data, reduced by the photometric pipeline (the  $i^*$  designation is used for preliminary SDSS photometry). The contours are drawn at intervals of 10% of the peak density of points. The redder stars extend to fainter magnitudes than do the bluer stars, due to the  $i^*$  limit.

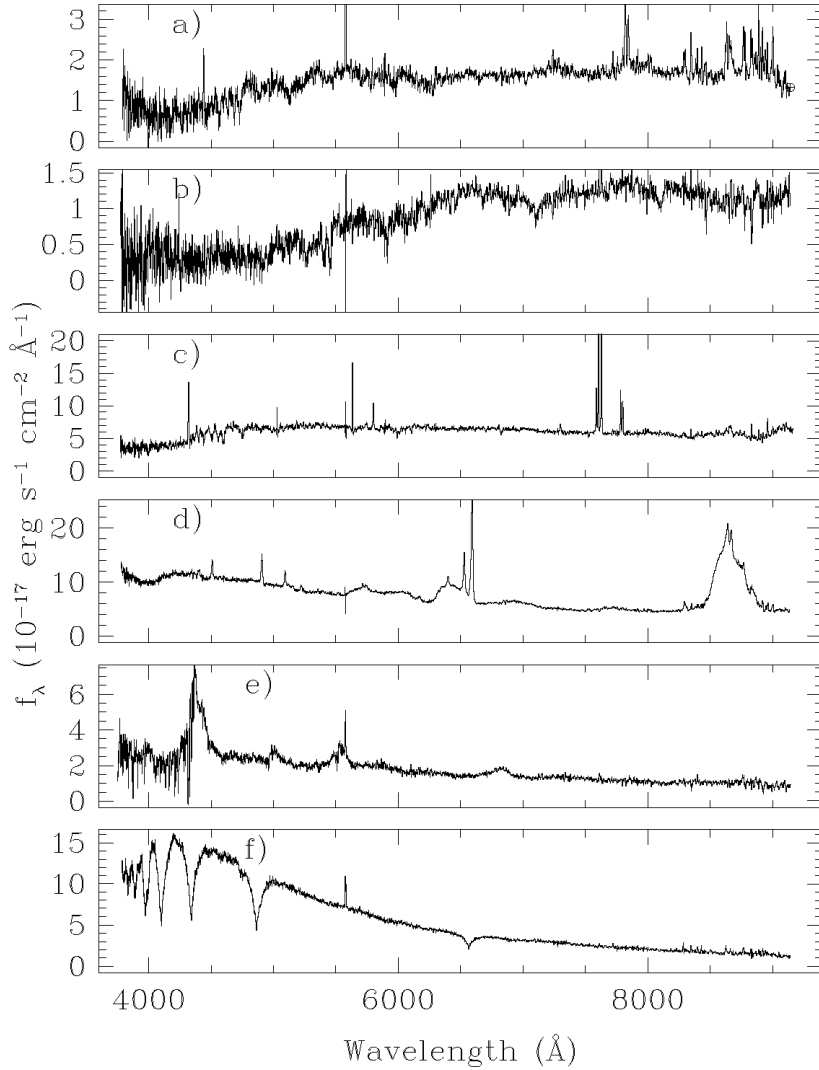


Figure 6. Representative SDSS spectra taken from a single spectroscopic plate observed on 4 October 1999 for a total of one hour of integration time, processed by the SDSS spectroscopic pipeline. For display purposes, all spectra have been smoothed with a 3-pixel boxcar function. All spectra show significant residuals due to the strong sky line at  $5577\text{\AA}$ . The objects depicted are: a. An  $r_p^* = 18.00$  galaxy;  $z = 0.1913$ . This object is slightly fainter than the main galaxy target selection limit. Note the  $H\alpha/[N\text{ II}]$  emission at  $\sim 7800\text{\AA}$ ,  $[O\text{ II}]$  emission at  $\sim 4450\text{\AA}$ , and Ca II H and K absorption at  $\sim 4700\text{\AA}$ . b. An  $r_p^* = 19.41$  galaxy,  $z = 0.3735$ . This object is close to the photometric limit of the Bright Red Galaxy sample. The H and K lines are particularly strong. c. A star-forming galaxy with  $r_p^* = 16.88$ , at  $z = 0.1582$ . d. A  $z = 0.3162$  quasar, with  $r_{psf}^* = 16.67$ . Note the unusual profile shape of the Balmer lines. This quasar is LBQS 0004+0036 (Morris et al. 1991). e. A  $z = 2.575$  quasar with  $r_{psf}^* = 19.04$ ; note the resolution of the Lyman- $\alpha$  forest. This quasar was discovered by Berger & Fringant (1985). f. A hot white dwarf, with  $r_{psf}^* = 18.09$ .

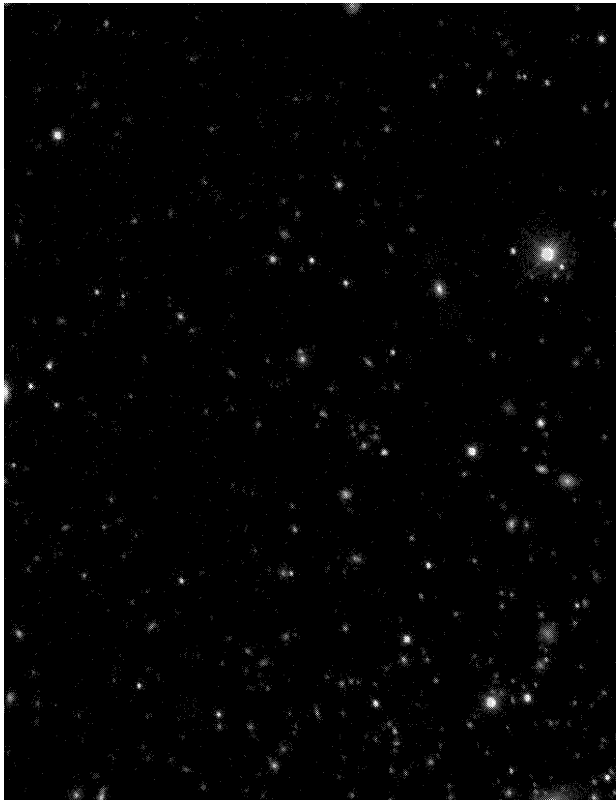


Figure 7. A sample frame ( $13' \times 9'$ ) from the SDSS imaging commissioning data. The image, a color composite made from the  $g'$ ,  $r'$ , and  $i'$  data, shows a field containing the distant cluster Abell 267 ( $\alpha = 01^h 52^m 41.0^s$ ,  $\delta = +01^\circ 00' 24.7''$ , redshift  $z = 0.23$ , Crawford et al. 1999); this is the cluster of galaxies with yellow colors in the lower center of the frame. The frame also contains, in the upper center, the nearby cluster RX J0153.2+0102, estimated redshift  $\sim 0.07$  (Bade et al. 1998) ( $\alpha = 01^h 53^m 15.15^s$ ,  $\delta = +01^\circ 02' 18.8''$ ). The psf (optics plus seeing) was about  $1.6''$ . Right ascension increases from bottom to top of the frame, declination from left to right.